

# Prins condensation for synthesis of nopol from $\beta$ -pinene and paraformaldehyde on novel Fe–Zn double metal cyanide solid acid catalyst

Mallikarjun V. Patil, Mukesh K. Yadav, Raksh V. Jasra\*

*Silicates and Catalysis Discipline, Central Salt and Marine Chemicals Research Institute (CSMCRI), G.B. Marg, Bhavnagar, Gujarat 364002, India*

Received 25 January 2007; received in revised form 16 March 2007; accepted 20 March 2007

Available online 25 March 2007

## Abstract

The present work describes the novel application of Fe–Zn double metal cyanide complexes as solid acid catalysts for the synthesis of nopol from  $\beta$ -pinene. The series of Fe–Zn double metal cyanide complexes were prepared from aqueous solutions of  $\text{ZnCl}_2$  and  $\text{K}_4\text{Fe}(\text{CN})_6 \cdot 3\text{H}_2\text{O}$  in the presence of *tert*-butanol, *iso*-butanol and *n*-butanol (complexing agent) and tri-block copolymer  $\text{EO}_{20}\text{PO}_{70}\text{EO}_{20}$  (average molecular weight, 5800; co-complexing agent). The catalysts prepared were characterized by X-ray diffraction, thermal analysis, diffuse reflectance UV–vis and FT-IR spectroscopy. All the catalysts were found to be active solid acid catalyst for Prins condensation reaction between paraformaldehyde and  $\beta$ -pinene in the synthesis of nopol. Coordinatively unsaturated  $\text{Zn}^{2+}$  ions in the framework of Fe–Zn double metal cyanide complexes are found to be possible active sites.

© 2007 Elsevier B.V. All rights reserved.

**Keywords:**  $\beta$ -pinene; Nopol; Prins condensation; Fe–Zn double metal cyanide (DMC) complexes

## 1. Introduction

Nopol is an optically active bicyclic primary alcohol used as a fragrance material in the manufacture of soaps, detergents, polishes and other household products. This also finds applications in agrochemical industry during the synthesis of pesticides. The conventional methods followed for its synthesis include Prins condensation of  $\beta$ -pinene and paraformaldehyde using zinc chloride as a catalyst at 115–120 °C for several hours with 57% yield of nopol, or employing acetic acid as a catalyst at 120 °C which yields nopylacetate which is then saponified to nopol or autoclaving a mixture of  $\beta$ -pinene and para formaldehyde at 150–230 °C for several hours yielding quantitative amounts of nopol [1]. All the above methods, in addition to nopol, also form monocyclic isomers and other side products. Furthermore, these homogeneous catalysts have drawbacks in terms of their corrosive nature, difficulty in separation from reaction products and post synthesis disposals and recov-

ery from the effluents. Therefore, research efforts are being directed to develop eco-friendly catalytic routes for the synthesis of nopol [2–6]. Pillai and Demessie have reported the synthesis of nopol over mesoporous iron phosphate catalyst in presence of acetonitrile as a solvent at 80 °C [2]. Villa de et al. have reported the synthesis of nopol over Sn-MCM-41 mesoporous molecular sieves in presence of toluene as a solvent at 90 °C [3,4]. More recently, mesoporous and microporous solid acid catalysts [5] as well as  $\text{ZnCl}_2$  impregnated Indian montmorillonite clay [6] have been reported as active catalysts for selective synthesis of nopol. Presently, there is increasing interest in developing clean chemical technologies which focus on the replacement of volatile organic solvents and achieving high atom economy. There is also a great demand to develop highly selective heterogeneous catalyst based technologies under mild conditions without employing toxic materials. Double metal cyanide (DMC) complexes are currently used as catalysts for the ring opening polymerization of epoxides, as well as coupling of epoxides and  $\text{CO}_2$  for manufacturing of biodegradable polycarbonates [7]. Recently, Srivastava et al. [8,9] have reported their application as a solid transesterification catalyst. In this contribution, we have evaluated the novel application of Fe–Zn

\* Corresponding author. Tel.: +91 278 2471793; fax: +91 278 2567562/66970.  
E-mail address: [rvjasra@csmcri.org](mailto:rvjasra@csmcri.org) (R.V. Jasra).

double metal cyanide (DMC) as a catalyst in selective synthesis of nopol.

## 2. Experimental

### 2.1. Chemicals

Potassium Ferrocyanide,  $K_4[Fe(CN)_6] \cdot 3H_2O$  from Polypharm Private Limited Bombay, India, and  $ZnCl_2$  from RANKEM, India, were used as the starting materials for the catalyst preparation, and *n*-butanol, *iso*-butanol and *tert*-butanol used as complexing agents were purchased from S.D. Fine Chemicals. Ltd., Bombay, India, Triblock copolymer, poly(ethylene glycol)-block-poly(propylene glycol)-block-poly(ethylene glycol) (Pluronic P123, molecular weight = 5800,  $EO_{20}PO_{70}EO_{20}$ ) was used as co-complexing agent and substrate  $\beta$ -pinene were procured from Sigma–Aldrich, USA, Paraformaldehyde was procured from National Chemicals, Vadodara, India. All the chemicals were used as such without further purification.

### 2.2. Catalyst preparation

In typical preparation of DMC-1 catalyst, 0.01 mol of potassium ferrocyanide (II)  $K_4[Fe(CN)_6] \cdot 3H_2O$  was dissolved in 40 mL of double distilled water to prepare solution 1. In a separate beaker, solution 2 was prepared by dissolving 0.1 mol of  $ZnCl_2$  in 100 mL of distilled water and 20 mL of *n*-butanol (complexing agent). Fifteen grams of tri-block copolymer (co-complexing agent) was dissolved in third beaker containing 2 mL of distilled water and 40 mL of *n*-butanol to prepare solution 3. Solution 2 was added to solution 1 slowly over 1 h at 323 K under vigorous stirring, a white solid was precipitated. Solution 3 was then added to the above reaction mixture over 5–10 min, and stirring was continued for another 1 h. The solid thus formed was filtered, washed thoroughly with double distilled water to remove all the uncomplexed ions, and dried at 298 K over night and the catalyst is designated as DMC-1. Similar synthesis procedure was employed for preparation of other DMC catalysts, with or without complexing and co-complexing agents as shown in Table 1. To study the effect of different alcohols as complexing agents on the catalytic activity, catalysts namely DMC-5, DMC-6 were prepared using similar method as of DMC-1 but complexing agents *iso*-butanol and *tert*-butanol were used, respectively [8–10,13]. To further study the effect

of co-complexing agent on catalyst composition and catalytic activity, catalysts with out tri-block copolymer (co-complexing agent) were prepared by adding *n*-butanol in case of DMC-2, *iso*-butanol for DMC-4 and *tert*-butanol in case of DMC-7, as complexing agents, respectively. Besides, we also studied the effect of absence of complexing and co-complexing agents on catalyst composition and its catalytic activity with DMC-3, prepared with similar method but without addition of any complexing and co-complexing agents. The details of the catalyst preparations are shown in Table 1.

### 2.3. Catalyst characterization

Structural analysis of  $ZnCl_2$ ,  $K_4[Fe(CN)_6] \cdot 3H_2O$  and Fe–Zn double metal cyanide complexes were done by X-ray diffraction using Philips X'PERT MPD diffractometer with  $Cu K\alpha_1$  ( $\lambda = 1.5405 \text{ \AA}$ ) as a radiation source in  $2\theta$  from 2 to  $80^\circ$ .

FT-IR Perkin-Elmer Spectrum GX FT-IR spectrophotometer was used for elucidating the bonding and functional group analysis of the prepared catalyst samples.

Diffuse reflectance spectroscopic (DRS) studies were carried out using Shimadzu UV-3101PC equipped with an integrating sphere.  $BaSO_4$  was used as the reference material.

The spectra were recorded at room temperature in the wavelength range of 200–800 nm.

The thermo gravimetric analysis was done on Mettler Toledo (TGA/SDTA851<sup>e</sup>) instrument with air flow ( $50 \text{ cm}^3/\text{min}$ ) with heating rate of 10 K/min in the temperature range of 323–923 K.

The surface morphological details of catalysts were studied by Scanning Electron Microscope (Leo 1430 VP) accelerated at 10 and 20 keV. The catalyst samples were mounted directly on the holders and covered with sputtered gold and then observed in SEM.

The  $N_2$  adsorption/desorption isotherms of samples were measured at 77.4 K using a gas sorption analyzer (Micromeritics ASAP 2010). The samples were degassed at 453 K for 4 h before the adsorption measurements. The specific surface area was calculated by the BET equation.

### 2.4. Catalytic studies

Known amounts of the catalyst (0.1–0.2 g) and reactant ( $\beta$ -pinene:paraformaldehyde = 5:10 mmol) were taken in 25 mL round bottom flask equipped with an efficient water condenser. The flask was kept in a constant temperature oil bath with the

Table 1  
Catalyst preparation and characteristics

Catalyst	Fe(II) precursor	Zn(II) precursor	Complexing agent	Co-complexing agent	BET surface area ( $\text{m}^2/\text{g}$ )
DMC-1	$K_4Fe(CN)_6 \cdot 3H_2O$	$ZnCl_2$	<i>n</i> -Butanol	$EO_{20}PO_{70}EO_{20}$	15
DMC-2	$K_4Fe(CN)_6 \cdot 3H_2O$	$ZnCl_2$	<i>n</i> -Butanol	Nil	154
DMC-3	$K_4Fe(CN)_6 \cdot 3H_2O$	$ZnCl_2$	Nil	Nil	229
DMC-4	$K_4Fe(CN)_6 \cdot 3H_2O$	$ZnCl_2$	<i>iso</i> -butanol	Nil	102
DMC-5	$K_4Fe(CN)_6 \cdot 3H_2O$	$ZnCl_2$	<i>iso</i> -butanol	$EO_{20}PO_{70}EO_{20}$	12
DMC-6	$K_4Fe(CN)_6 \cdot 3H_2O$	$ZnCl_2$	<i>tert</i> -Butanol	$EO_{20}PO_{70}EO_{20}$	7
DMC-7	$K_4Fe(CN)_6 \cdot 3H_2O$	$ZnCl_2$	<i>tert</i> -Butanol	Nil	47

temperature maintained at  $353 \pm 2$  K using PID temperature controller under continuous 500 rpm magnetic stirring for 12 h. The reaction mixture was centrifuged and the organic products were analyzed by gas chromatograph (Hewlett-Packard, Model-6890), equipped with HP-5 capillary column (30 m long and 0.32 mm internal diameter) with flame ionization detector. The oven temperature was programmed at the rate of  $5^\circ \text{ min}^{-1}$  in temperature range of 343–492 K. High purity  $\text{N}_2$  gas was used (flow rate of 30 mL/h) as a carrier gas for analysis. Pure standard reagents were used for the product determination and identification. The calibration of GC peak areas was carried out by taking solutions of known compositions with dodecane as an internal standard. Product identification is also done by gas chromatograph/mass spectrometer (Shimadzu GCMS-QP-2010, Japan) with GC oven programmed in the temperature range 313–492 K and helium as a carrier gas and MS in EI mode with 70 eV ion source. The conversion and selectivity was calculated as follows.

$$\text{conversion (mol\%)} = \frac{(\text{initial mol\%} - \text{final mol\%})}{\text{initial mol\%}} \times 100$$

$$\text{selectivity of product} = \frac{\text{GC peak area of desired product}}{\sum \text{GC peak area of all products}} \times 100$$

Percentage error in GC analysis was  $\pm 1\%$

### 3. Results and discussion

#### 3.1. Characterization of double metal cyanide complex catalysts

Fig. 1 shows X-ray diffractograms of powdered Fe–Zn double metal cyanide complexes and their precursor compounds,  $\text{K}_4[\text{Fe}(\text{CN})_6] \cdot 3\text{H}_2\text{O}$  and  $\text{ZnCl}_2$ . The sharp peaks in the XRD pattern for Fe–Zn double metal cyanide complexes reveal that the catalysts are highly crystalline and contain negligible quantities of the starting compounds,  $\text{K}_4[\text{Fe}(\text{CN})_6] \cdot 3\text{H}_2\text{O}$  and  $\text{ZnCl}_2$ . Peak

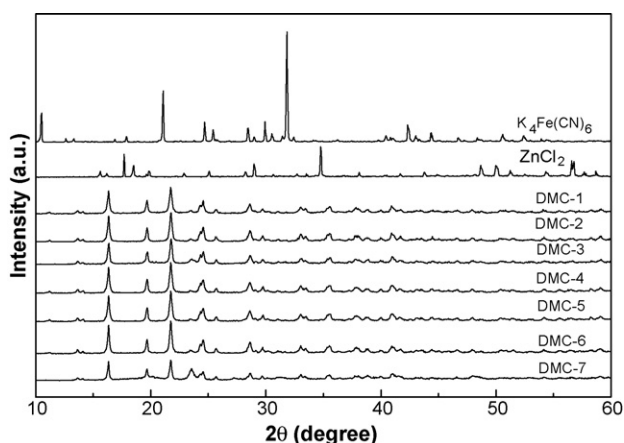


Fig. 1. XRD pattern of precursor compounds  $\text{K}_4[\text{Fe}(\text{CN})_6] \cdot 3\text{H}_2\text{O}$ ,  $\text{ZnCl}_2$  and Fe–Zn double metal cyanide complexes.

indexing has revealed that all the Fe–Zn double metal cyanide complexes crystallize in cubic lattice [11], with an unit cell parameter 0.904 nm. XRD patterns of all Fe–Zn double metal cyanide complexes (Fig. 1) are similar, except that the crystallinity of the Fe–Zn double metal cyanide complexes which were prepared in absence of complexing and co-complexing agents is higher. Small difference in  $2\theta$  values for Fe–Zn double metal cyanide complexes are most likely due to differences in the number of coordinated water and alcoholic molecules (Fig. 1). The XRD pattern of the DMC-1 catalyst is characterized by the following peaks:  $2\theta$  ( $hkl$ )— $16.3^\circ$  (1 1 1),  $19.6^\circ$  (2 0 0),  $21.7^\circ$  (2 1 0),  $24.5^\circ$  (2 1 1), and  $28.6^\circ$  (2 2 1).

IR spectroscopy is an ideal technique for differentiating the various coordination modes of cyanide groups in metal complexes. Except for the peaks due to coordinated water molecules,  $\text{ZnCl}_2$  showed no additional IR bands in the spectral region of  $4000\text{--}400 \text{ cm}^{-1}$ .  $\text{K}_4[\text{Fe}(\text{CN})_6] \cdot 3\text{H}_2\text{O}$  showed an intense characteristic band at  $2045 \text{ cm}^{-1}$  due to  $\nu(\text{C}\equiv\text{N})$ , which shifted to  $2097 \text{ cm}^{-1}$  for the Fe–Zn double metal cyanide complexes (Fig. 2). The free cyanide ion showed band at  $2080 \text{ cm}^{-1}$  [12]. Earlier studies [13–19] reported a similar shift in the position of this band to higher frequencies in related double metal cyanide catalysts; for example, Co–Zn double metal cyanides exhibited a shift of this band to  $2196 \text{ cm}^{-1}$  from  $2133 \text{ cm}^{-1}$ , corresponding to the precursor compound,  $\text{K}_3\text{Co}(\text{CN})_6$  [13]. In the case of  $\text{Fe}^{3+}\text{--Zn}^{2+}$  catalyst, this band appeared at  $2179 \text{ cm}^{-1}$  [14]. Multimetal cyanides ( $\text{Co}^{3+}\text{--Fe}^{2+}\text{--Zn}^{2+}$ ) absorb at  $2101 \text{ cm}^{-1}$  [14]. The  $\nu(\text{C}\equiv\text{N})$  values for the metal complexes are generally higher than those for free  $\text{CN}^-$ . The shift of this band from  $2045 \text{ cm}^{-1}$  for  $\text{K}_4[\text{Fe}(\text{CN})_6] \cdot 3\text{H}_2\text{O}$  to  $2097 \text{ cm}^{-1}$  (for Fe–Zn double metal cyanide complexes) in the present study suggests the formation of a new mixed-metal complex of ferrocyanide moiety and  $\text{Zn}^{2+}$  ions by means of bridging cyanide ligands [20]. Cyanide ions act not only as  $\sigma$ -donors (by donating electrons to Fe), but also as  $\pi$ -donors (by chelating to Zn). Electron donation raises the  $\nu(\text{CN})$ , because electrons are removed from the  $5\sigma$  orbital, which is weakly antibonding.

Consequently, the  $\nu(\text{C}\equiv\text{N})$  band shifts to higher frequencies;  $\pi$ -back-bonding tends to decrease the  $\nu(\text{CN})$ , because the

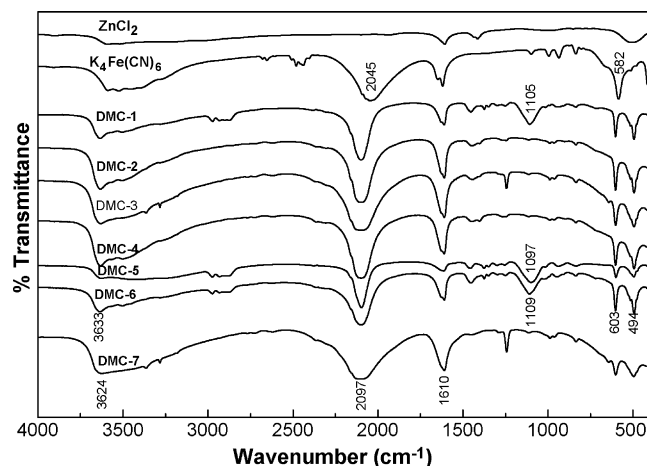
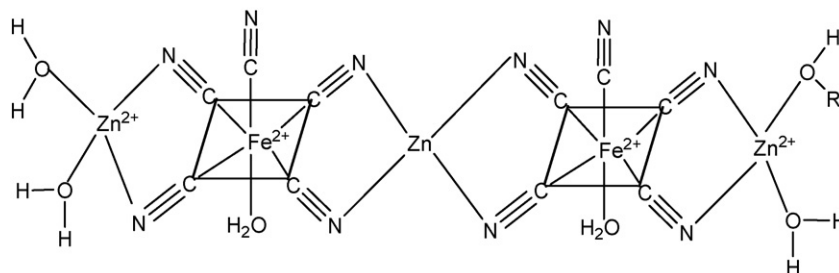


Fig. 2. FT-IR spectra of  $\text{ZnCl}_2$ ,  $\text{K}_4[\text{Fe}(\text{CN})_6]$  and Fe–Zn double metal cyanide complexes.



Scheme 1. Tentative structure of double metal cyanide Fe–Zn complex.

electrons enter into the anti-bonding  $2p\pi^*$  orbital. In general,  $\text{CN}^-$  is a good  $\sigma$ -donor and a poor  $\pi$ -acceptor. Thus,  $\nu(\text{CN})$  for the complexes is generally higher than the values for free  $\text{CN}^-$ . IR spectra also suggest that the cyanide ligands are oriented linearly between the divalent  $\text{Zn}^{2+}$  and  $\text{Fe}^{2+}$ , with the C atom possibly coordinated to  $\text{Fe}^{2+}$ . The analogous cyano-bridged  $[\text{CpFe}(\text{PPh}_3)(\mu\text{-CN})_2\text{ZnI}(\text{CH}_3\text{CN})]_2$  complex shows characteristic  $\nu(\text{CN})$  bands at  $2092$  and  $2082\text{ cm}^{-1}$  [20], confirming that cyano bridging exists between the  $\text{Fe}^{2+}$  and  $\text{Zn}^{2+}$  moieties in the complexes of the present study. All Fe–Zn double metal cyanide complexes catalysts (DMC-1, DMC-2, DMC-3, DMC-4, DMC-5, DMC-6, and DMC-7) showed  $\nu(\text{CN})$  bands at identical positions, indicating that the method of preparation did not influence the primary structure of the Fe–(CN) $_n$ –Zn moiety. Fig. 2 shows additional bands at  $3633$ ,  $3424$ ,  $1610$ ,  $1109$ ,  $603$ , and  $494\text{ cm}^{-1}$  and weak bands in the  $1100$ – $800\text{ cm}^{-1}$  region confirm the presence of water molecules and coordinated alcoholic group ( $1105$ ,  $1097$  and  $1109\text{ cm}^{-1}$ ) in DMC-1, DMC-5 and DMC-6, respectively. Absence of the band at  $1105$ ,  $1097$  and  $1109\text{ cm}^{-1}$  (as well as any band in the  $2800$ – $3000\text{ cm}^{-1}$  region) in the spectra of DMC-2, DMC-3, DMC-4, and DMC-7 shows the absence of alcoholic group in their structures. The tentative structure of double metal cyanide Fe–Zn complex is given in Scheme 1.

$\text{ZnCl}_2$  showed no UV–vis peaks in the region of  $200$ – $800\text{ nm}$ .  $\text{K}_4\text{Fe}(\text{CN})_6 \cdot 3\text{H}_2\text{O}$ , prussian-blue crystalline complex showed spectral minima around  $245$ ,  $278$  and  $330\text{ nm}$  in the UV region (Fig. 3). The peak at  $245\text{ nm}$  is assigned to the  $\pi$ – $\pi^*$  charge transfer transitions in the CN ligand, whereas the latter two peaks are assigned to the ligand-to-metal (Fe) charge transfer (LMCT) transitions [8]. UV–vis DRS spectra of various Fe–Zn double metal cyanide catalysts show LMCT peaks shifted to the higher energy side at  $266$  and  $315\text{ nm}$ , respectively. This is probably due to donation of antibonding electron to both  $\text{Fe}^{2+}$  and  $\text{Zn}^{2+}$  ions. These data give additional support to the observation made from FT-IR results, which confirm that Fe–Zn double metal cyanide complexes contain the bridging cyano groups between Fe and Zn. No additional peaks were observed for  $\text{K}_4\text{Fe}(\text{CN})_6 \cdot 3\text{H}_2\text{O}$  and Fe–Zn double metal cyanide complexes in visible region, indicating that Fe, in the Fe–Zn DMC catalysts, is in low spin  $+2$  oxidation state corresponding to  $^1A_{1g}$  ground state. The electronic transition from  $^1A_{1g}$  to excited triplet state is Laporte forbidden and hence no d–d transitions were observed in the visible region.

Surface area values for the various catalysts given in Table 1 show that the catalysts (DMC-1, DMC-5 and DMC-6) prepared using tri-block copolymer as a co-complexing agent and alcohols as complexing agent have very low surface area ( $7$ – $15\text{ m}^2/\text{g}$ ). On the other hand, catalysts (DMC-2, DMC-4 and DMC-7) prepared using only complexing agent show higher surface areas ( $47$ – $154\text{ m}^2/\text{g}$ ). It is interesting to observe that the surface values show decreasing trend with an increase in alkyl chain branching of butanol. The catalysts prepared without using complexing and co-complexing agent (DMC-3) showed the highest surface area ( $229\text{ m}^2/\text{g}$ ). These observations can be explained in terms of the accessibility of mesopores to nitrogen molecules in these catalysts. In catalyst samples prepared using both complexing and co-complexing agents, the mesopores formed during precipitation of double metal cyanide complexes are occupied by the molecules of tri-block copolymer and alcohol leading to less accessibility to nitrogen molecules. The increased surface area values in samples prepared without using co-complexing triblock copolymer can be explained in terms of increased mesoporous volume as mesopores are occupied only by alcohol molecules. The observation that surface area decreases with increasing alkyl chain branching is also explained in terms of increased occupancy of mesopores by branched alcohols compared to normal alcohol. For the sample prepared without using complexing and co-complexing agent, mesopores are fully accessible to nitrogen molecules

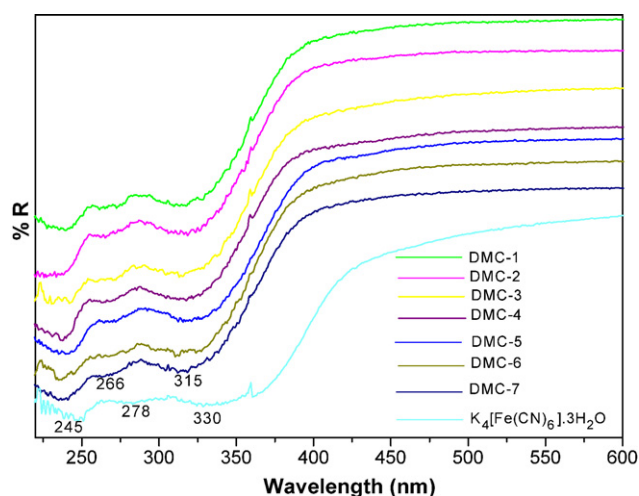


Fig. 3. Diffuse reflectance UV–vis spectra of Fe–Zn double metal cyanide complexes.

used for surface area measurement leading to highest surface area.

Thermal stability of the Fe–Zn double metal cyanide complex catalysts was investigated using TGA. On calcinations in air for 4 h, DMC-1 retained its characteristic crystalline structure up to 473 K. Thermal analysis data show three stage of weight loss: stage I (at 323–573 K), stage II (at 573–656 K), and stage III (at 823–1073 K). Stage I consequent to desorption of the water and complexing agents (alcohol) molecules; stage II is due to decomposition of the cyanide group, followed by transformation of the DMC complexes into metal nitrates and carbonates; and stage III is attributed to the complete decomposition of the material into the metal oxides ZnFeO<sub>4</sub> and ZnO [8].

The scanning electron micrographs of the catalyst materials (Fe–Zn double metal cyanide complexes) as shown in Fig. 4, illustrate that catalyst particle for DMC-5, DMC-6 and DMC-7 prepared using *iso*-butanol and *tert*-butanol as complexing and EO<sub>20</sub>PO<sub>70</sub>EO<sub>20</sub> as co-complexing agent have spherical morphology with the particle size of the catalyst in the range of 1–3 μm. The other catalysts showed agglomeration of catalyst particles.

### 3.2. Catalytic activity of catalysts

Tables 2–4 show the data on conversion of β-pinene and selectivity of nopol over different Fe–Zn double metal cyanide complex catalysts.

It is observed from Table 2 that the Fe–Zn double metal cyanide catalysts show conversion of β-pinene in the range of 25–31 with nopol selectivity varying from 50 to 85. The other products formed in addition to nopol include pinocarveol, pinocarvone, myrtenal and myrtenol as determined by GCMS analysis of the reaction products given in Fig. 5. The mass data showed standard fragmentation pattern corresponding to nopol (*m/z*: 166, 122, 105, 91, 79, 41) pinocarveol (*m/z*: 152, 135, 119, 109, 92, 83, 55, 41) pinocarvone (*m/z*: 150, 122, 108, 91, 81, 69,

Table 2

Nopol synthesis by Prins condensation of β-pinene and paraformaldehyde over Fe–Zn double metal cyanide complex catalyst<sup>a</sup>

Entry	Catalyst	%Conversion	%Selectivity				
			A	B	C	D	E
1	DMC-1	29	4	6	13	7	69
2	DMC-2	26	7	7	17	10	53
3	DMC-3	25	9	11	18	11	50
4	DMC-4	27	8	6	16	10	55
5	DMC-5	30	3	3	5	6	78
6	DMC-6	31	3	3	4	4	85
7	DMC-7	30	5	9	16	8	58
8	Nil	00	–	–	–	–	–

<sup>a</sup>Reaction conditions: β-pinene:paraformaldehyde = 5:10 mmol; catalyst, 0.1 g; time = 12 h; temperature = 353 K. A, pinocarveol; B, pinocarvone; C, myrtenal; D, myrtenol; E, nopol.

53) myrtenal (*m/z*: 150, 135, 107, 93, 91, 79, 41) and myrtenol (*m/z*: 152, 119, 108, 93, 91, 79, 41).

It is also observed that the catalysts prepared without complexing and co-complexing agent gives the least conversion and nopol selectivity (entry 3, Table 2). It is further seen from the data that catalysts prepared using both complexing and co-complexing agents (entries 1 and 5–6 in Table 2) show higher conversion and nopol selectivity compared to those where only complexing agent was used (entries 2, 4, 7 in Table 2). The order of β-pinene conversion and nopol selectivity observed for catalyst prepared using EO<sub>20</sub>PO<sub>70</sub>EO<sub>20</sub> as co-complexing agent is dependent on the nature of complexing agent. Though, conversion has small variation (29–31%), the nopol selectivity shows significant variation in the following order, *tert*-butanol (85%) > *iso*-butanol (78%) > *n*-butanol (69%). This is attributed to the presence of more Lewis acidic sites (Zn<sup>+2</sup>, Scheme 1) in the catalysts having complexing agents as well as co-complexing agents as mentioned in literature [8,9] from measurement of surface acidity from pyridine adsorption using temperature programmed desorption (TPD) and DRFIT spectroscopy. We also

Table 3

Effect of reaction temperature, catalyst activation, solvent addition, catalyst amount and reaction time

Entry	Catalyst	Temperature (K)	Time (h)	Conversion (%)	Selectivity (%)				
					A	B	C	D	E
1	DMC-6	333	12	3	7	6	6	5	76
2	DMC-6	373	12	26	1	2	4	2	88
3	DMC-6 <sup>a</sup>	353	12	31	1	2	4	2	90
4	DMC-6 <sup>b</sup>	353	12	8	–	4	2	1	92
5	DMC-6 <sup>c</sup>	353	12	10	–	4	2	1	90
6	DMC-6 <sup>d</sup>	353	12	25	7	9	15	11	52
7	DMC-6 <sup>e</sup>	353	12	48	3	3	3	4	85
8	DMC-6 <sup>f</sup>	353	12	24	6	8	12	9	60
9	DMC-6	353	24	45	5	6	12	7	67

Reaction conditions: β-pinene:paraformaldehyde = 5:10 mmol; catalyst, 0.1 g; time = 12 h. A, pinocarveol; B, pinocarvone; C, myrtenal; D, myrtenol; E, nopol.

<sup>a</sup> Catalyst pre-activated (453 K for 4 h).

<sup>b</sup> Acetonitrile, 10 mL (substrate to solvent molar ratio, 1:36).

<sup>c</sup> Toluene, 10 mL (substrate to solvent molar ratio, 1:18).

<sup>d</sup> Paraformaldehyde, 5 mmol.

<sup>e</sup> Catalyst, 0.2 g.

<sup>f</sup> Catalyst, 0.05 g.

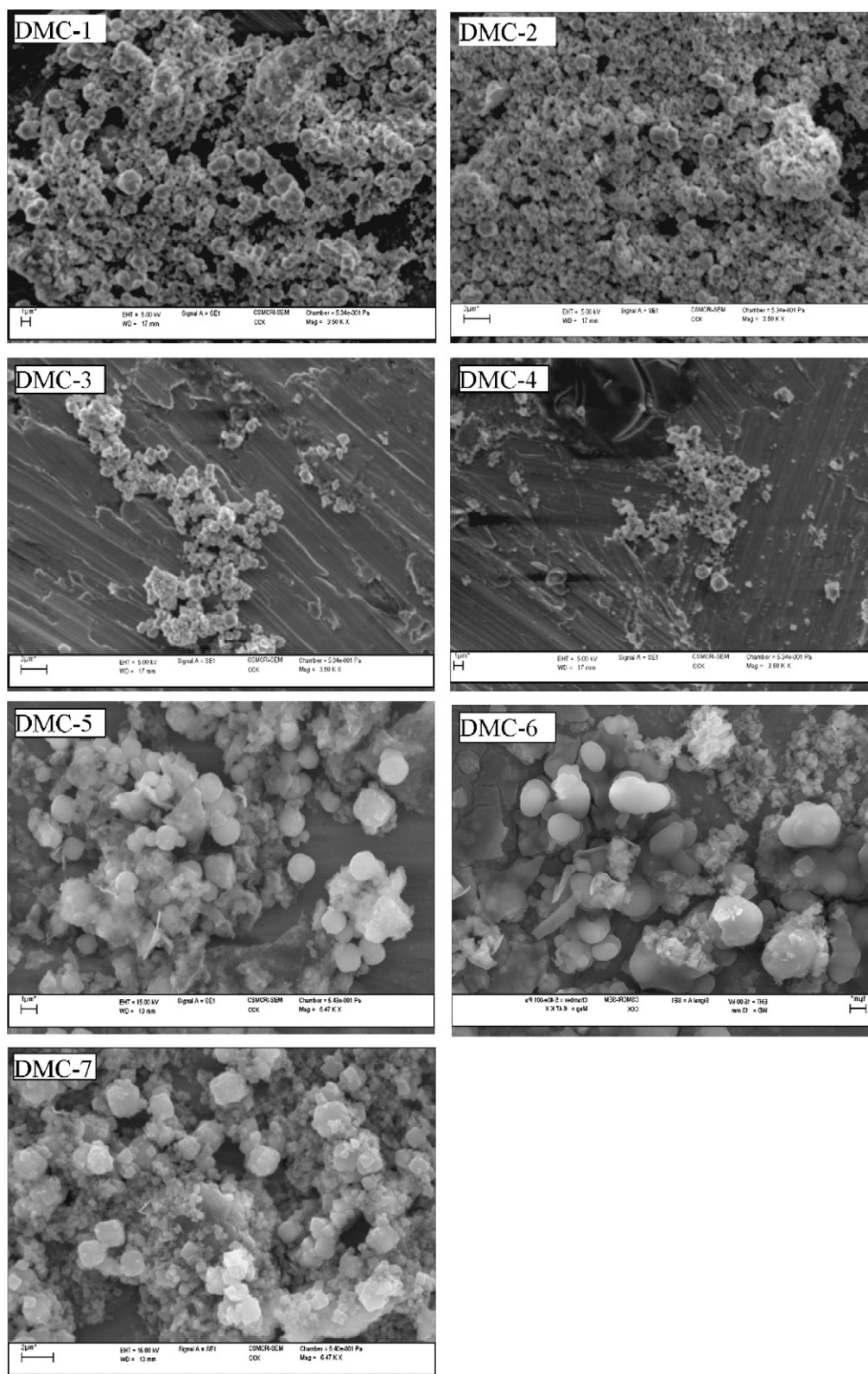


Fig. 4. SEM images of (Fe-Zn double metal cyanide complex) catalysts.

observed that in the absence of catalyst there was no conversion of  $\beta$ -pinene (entry 8 in Table 2).

As catalyst DMC-6 has shown the highest catalytic activity, this was selected as a representative catalyst for the further study.

The effect of experimental conditions namely catalyst activation, nature of the solvents, catalyst amount, reaction temperature and time were studied and the data are shown in Table 3. Effect of reaction temperature study showed that at 333 K no significant

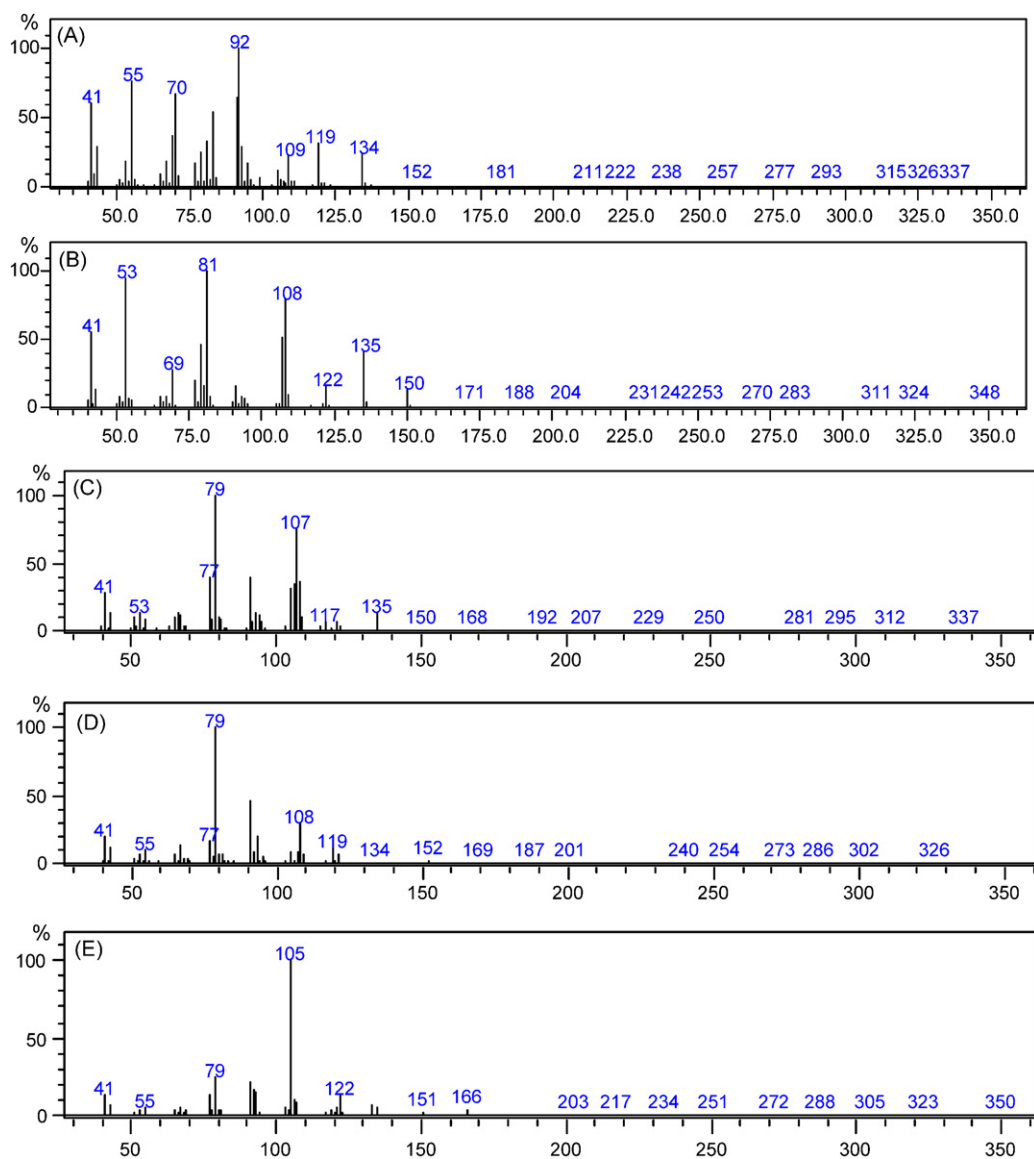


Fig. 5. Mass fragmentation pattern A, pinocarveol; B, pinocarvone; C, myrtenal; D, myrtenol; E, nopol.

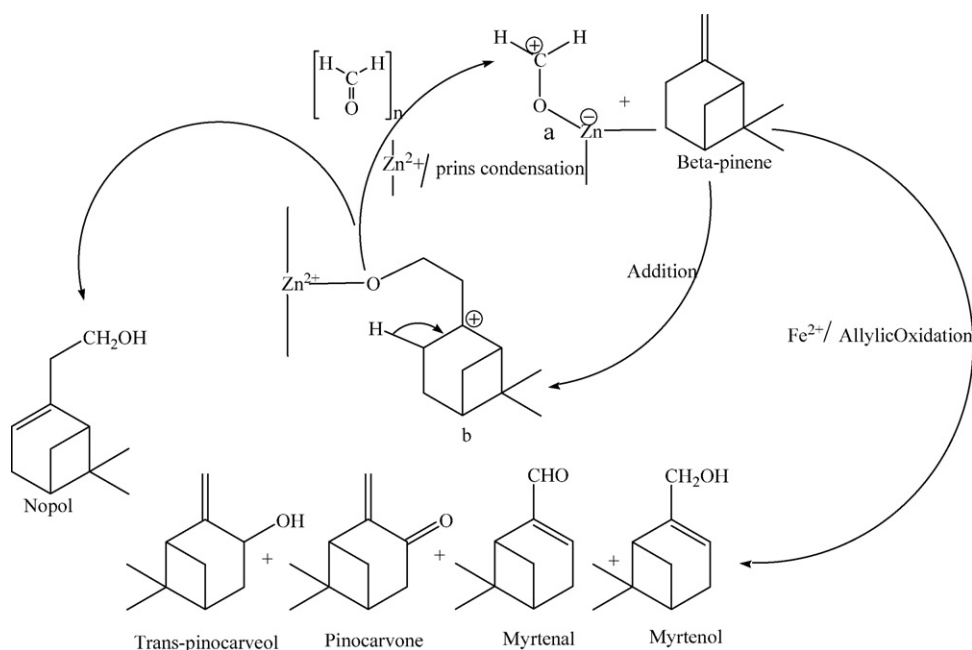
conversion was observed probably due to insufficient formation of formaldehyde molecules from paraformaldehyde, as the temperature was increased to 373 K  $\beta$ -pinene conversion increased to 26% with 88% nopol selectivity (entries 1–2, Table 3). But best results were observed at 353 K where 31%  $\beta$ -pinene conversion was obtained with 85% nopol selectivity (entry 6, Table 2). Therefore, most of the reactions were studied at 353 K. The activation of catalysts was carried out at 453 K for 4 h in a furnace in presence of air. The comparison of conversion and nopol selectivity determined with the catalyst used without activation showed no change in  $\beta$ -pinene conversion but 5% increase in nopol selectivity was observed with activated catalyst (entry 3, Table 3 and entry 6, Table 2).

From the data in Tables 1 and 2,  $\beta$ -pinene conversion and nopol selectivity are observed to decrease with the increase in surface area of the catalyst. However, this effect is more pronounced in selectivity values where exponential increase in nopol selectivity is observed for catalyst having surface area

Table 4  
Effect of acetonitrile amount on product distribution

Entry	Substrate:solvent (molar ratio)	%Conversion	%Selectivity	
			Nopol	Others
1	1:4	43	95	5
2	1:8	52	96	4
3	1:12	49	96	4
4	1:16	30	95	5
5	1:20	23	96	4
6	1:24	18	96	4
7	1:28	17	95	5
8	1:32	15	96	4

Reaction conditions:  $\beta$ -pinene:paraformaldehyde = 5:10 mmol; catalyst (DMC-6) = 0.1 g; time = 12 h; temperature = 353 K. Others: A, pinocarveol; B, pinocarvone; C, myrtenal; D, myrtenol; E, nopyl acetate; F, *trans*-caryophyllene.

Scheme 2. Tentative reaction mechanism for Prins condensation of  $\beta$ -pinene.

less than 50 m<sup>2</sup>/g. The proposed structure of the catalyst given in Scheme 1 shows catalytically active sites, namely coordinatively unsaturated Zn<sup>2+</sup> ions present on the extremities of the catalyst particles. Therefore, in the catalyst samples having lower surface areas due to occupancy of mesopores by complexing and co-complexing agents, the availability or accessibility of these active sites is minimally affected as these sites are present on the external surface rather than pores of the catalyst. As a result, the effect on  $\beta$ -pinene conversion with variation in the catalyst surface is not significant. The pronounced decrease in the nopol selectivity with increase in surface area of the catalysts can be explained in terms of enhanced accessibility of mesopores surface and thereby to Fe<sup>2+</sup> sites present in the mesopores to the  $\beta$ -pinene due to which  $\beta$ -pinene molecules get oxidized to products like pinocarveol, pinocarvone, myrtenal and myrtenol. This explanation is in consonance with the proposed catalyst structure (Scheme 1) and proposed reaction mechanism (Scheme 2).

To study the effect of polarity of the solvent, reactions were conducted with two solvents with substrate to solvent molar ratio 1:36 acetonitrile (polar) and 1:18 toluene (nonpolar) (entries 4–5, Table 3). Effect of paraformaldehyde to  $\beta$ -pinene molar ratio was done (entry 6, Table 3) and with 1:1 molar ratio both conversion and selectivity decreased. Increase in the catalyst amount was found to increase the  $\beta$ -pinene conversion probably due to availability of more number of catalytically active sites (entries 7–8, Table 3) and vice versa. Even increase in reaction time from 12 to 24 h was observed to show decrease in nopol selectivity (entry 9, Table 3) with increased formation of side products like pinocarveol, pinocarvone, myrtenal and myrtenol.

To further understand the effect of the solvent, molar ratio of  $\beta$ -pinene to solvent acetonitrile was varied from 1:4 to 1:32. The data given in Table 4 show increase in  $\beta$ -pinene conversion from 31 to 51% with  $\beta$ -pinene to solvent molar ratio of 1:8 beyond which conversion shows a sharp decrease. Nopol selectivity increases to 96% in the presence of the solvent compared

Table 5  
Effect of toluene amount on product distribution

Entry	Substrate:solvent (molar ratio)	Conversion (%)	Selectivity (%)						
			A	B	C	D	E	F	G
1	1:2	31	6	7	12	10	51	4	1
2	1:4	25	5	7	13	10	49	6	1
3	1:6	26	5	8	13	10	50	6	1
4	1:8	24	5	7	13	11	53	7	1
5	1:10	15	4	8	12	9	60	6	–
6	1:12	14	5	8	8	12	56	7	–
7	1:14	11	4	5	9	9	66	4	–
8	1:16	10	5	6	9	9	71	4	–

Reaction conditions:  $\beta$ -pinene:paraformaldehyde = 5:10 mmol; catalyst (DMC-6) = 0.1 g; time = 12 h; temperature = 353 K. A, pinocarveol; B, pinocarvone; C, myrtenal; D, myrtenol; E, nopol; F, perilla alcohol; G, nopyl acetate.



Table 6  
Performance of recycled DMC-6 catalyst

Entry	Recycle	Conversion (%)	Selectivity (%)				
			A	B	C	D	E
1	Initial	31	3	3	4	4	85
2	I	30	3	6	12	7	70
3	II	27	5	6	12	7	65
4	III	25	5	7	13	8	59

Reaction conditions:  $\beta$ -pinene:paraformaldehyde = 5:10 mmol; catalyst, 0.1 g; time = 12 h; temperature = 353 K. A, pinocarveol; B, pinocarvone; C, myrtenal; D, myrtenol; E, nopol.

to the value of 85% observed without solvent under similar conditions. However, nopol selectivity is not affected by the change in  $\beta$ -pinene to solvent molar ratio. The effect of  $\beta$ -pinene to solvent molar ratio (1:2–1:16) was also studied with toluene as a solvent. The data given in Tables 2 and 5 show no change in  $\beta$ -pinene conversion in the presence of solvent up to  $\beta$ -pinene to solvent molar ratio of 1:2 compared to conversion value obtained under solvent free conditions. However, beyond this molar ratio,  $\beta$ -pinene conversion showed a sharp decrease. However, up to  $\beta$ -pinene to solvent molar ratio of 1:2, nopol selectivity was observed to decrease to 51% compared with the value of 85% observed in solvent free conditions. However, at higher  $\beta$ -pinene to solvent molar ratios, nopol selectivity increased from 51 to 71%. The conversion was observed to be higher when acetonitrile was used as a solvent compared to toluene. This shows that polarity of the solvent (dielectric constant of acetonitrile is 37.5 and toluene is 2.4 at 20 °C) plays a role on the conversion.

The reusability of the catalyst was also studied as shown in Table 6. For reusability studies, after completion of reaction, catalyst was filtered and washed with methanol followed by acetone and dried at room temperature. It was found that the catalyst is reusable with minor decrease in conversion and selectivity which could be ascribed to handling loss of the catalyst.

### 3.3. Reaction mechanism

The mechanisms for Fe–Zn double metal cyanide catalyzed transesterification of dimethylcarbonate [8] and ring-opening polymerization of propylene oxide [14] were previously reported. A similar reaction pathway is proposed in the present case. Coordinatively unsaturated  $Zn^{2+}$  ions in the structure of Fe–Zn double metal cyanide complexes (Scheme 1) are the probable active sites which assist in the formation of species [a]. This is followed by the reaction of these species [a] with the  $\beta$ -pinene. This was followed by allylic proton transfer from  $\beta$ -pinene which results into the formation of unsaturated alcohol (nopol). A tentative mechanism over active Lewis acidic  $Zn^{2+}$  cations in the Fe–Zn double metal cyanide complex catalyst is shown in (Scheme 2). The variation observed in the conversion of  $\beta$ -pinene to nopol with acetonitrile to  $\beta$ -pinene molar ratio can be explained in terms of this mechanism. Acetonitrile being a polar molecule is expected to stabilize the polar carbonation, through interaction of positively charged species with nitrogen lone pair electrons and thereby enhancing the conversion. How-

ever, at higher acetonitrile to  $\beta$ -pinene molar ratio, acetonitrile molecules start competing with formaldehyde molecules for their interaction with catalytically active  $Zn^{2+}$  ions of the catalyst and thereby blocking the active sites which will result into decrease in conversion of  $\beta$ -pinene.  $Fe^{2+}$  ions are known to be active sites for allylic oxidation of beta-pinene. Thus, formation of allylic oxidation products, namely pinocarveol, pinocarvone, myrtenal and myrtenol could be possible due to the presence of  $Fe^{2+}$  in the  $Fe^{2+}$ – $Zn^{2+}$ -double metal cyanide complexes [21].

## 4. Conclusions

A novel application of double metal cyanide (DMC) complexes as highly active heterogeneous catalysts for synthesis of nopol from  $\beta$ -pinene and paraformaldehyde by Prins condensation reaction is reported. A catalyst containing of  $Fe^{2+}$ – $Zn^{2+}$  *tert*-butanol (DMC-6) was found to be superior to others. The method of catalyst preparation influences significantly the catalytic properties of the material. The use of surfactant molecules in synthesis is observed to enhance the catalytic activity. The Fe–Zn catalyst is reusable with little loss in activity. The accessible and Lewis acidic  $Zn^{2+}$  cations are the possible active sites in Prins condensation reaction.

## Acknowledgements

Authors are highly thankful to Council of Scientific and Industrial Research, India for financial support through Network Program on Catalysis and Dr. P.K. Ghosh, Director, CSMCRI, Bhubaneswar, India, for encouragement of this publication.

## References

- [1] J.P. Bain, J. Am. Chem. Soc. 68 (1946) 638.
- [2] U.R. Pillai, E.S. Demessie, Chem. Commun. (2004) 826.
- [3] A.L. Villa de P, E. Alarcón, C. Monetes de C, Chem. Commun. (2002) 2654.
- [4] A.L. Villa de P, E. Alarcón, C. Monetes de C, Catal. Today 107–108 (2005) 942.
- [5] M. Selvaraj, S. Kawi, J. Mol. Catal. A: Chem. 246 (2006) 218.
- [6] M.K. Yadav, R.V. Jasra, Catal. Commun. 7 (2006) 891.
- [7] I. Kim, M.J. Yi, S.H. Byun, D.W. Park, B.U. Kim, C.S. Ha, Macromol. Symp. 224 (2005) 181.
- [8] R. Srivastava, D. Srinivas, P. Ratnasamy, J. Catal. 241 (2006) 34.
- [9] P.S. Sreeprasanth, R. Srivastava, D. Srinivas, P. Ratnasamy, Appl. Catal. A: Gen. 314 (2006) 148.
- [10] H. Liu, X. Wang, Y. Gu, W. Guo, Molecules 8 (2003) 67.
- [11] S. Chen, P. Zhang, L. Chen, Prog. Org. Coat. 50 (2004) 269.
- [12] K. Nakamoto, Infrared Spectra of Inorganic and Coordination Compounds, John Wiley, New York, 1963, p. 167.
- [13] I. Kim, J.T. Ahn, S.H. Lee, C.S. Ha, D.W. Park, Catal. Today 93–95 (2004) 511.
- [14] I. Kim, J.T. Ahn, C.S. Ha, C.S. Yang, I. Park, Polymer 44 (2003) 3417.
- [15] M.O. James, L.L. Donald, L.G. Robin, US Patent 6,359,101 (2002).
- [16] K.G. McDaniel, M.J. Perry, J.E. Hayes, WO 9,914,258 (1999).
- [17] H. van der Hulst, G.A. Pogany, J. Kuyper, US Patent 4,477,589 (1984).
- [18] J. Milgrom, US Patent 3,404,109 (1968).
- [19] R.J. Herold, US Patent 3,278,459 (1966).
- [20] D.J. Darensbourg, M.J. Adams, C. Yarbrough, Inorg. Chem. 40 (2001).
- [21] L. Menini, M.J. da Silva, M.F.F. Lelis, J.D. Fabris, R.M. Lago, E.V. Gusevskaya, Appl. Catal. A: Gen. 269 (2004) 117.